Contribution of nitrogen atoms and ions to the luminescence emission during femtosecond filamentation in air

Su-Yu Li, Shu-Chang Li, Lai-Zhi Sui, Yuan-Fei Jiang, An-Min Chen,* and Ming-Xing Jin†
Institute of Atomic and Molecular Physics, Jilin University, Changchun 130012, China
and Jilin Provincial Key Laboratory of Applied Atomic and Molecular Spectroscopy (Jilin University), Changchun 130012, China
(Received 23 September 2015; published 8 January 2016)

During femtosecond filamentation in air, nitrogen molecules and corresponding molecular ions undergo dissociation due to the high intensity of laser pulses, generating nitrogen atoms and atomic ions. The generated atoms and atomic ions emit luminescence in the UV range, which superposes on those emissions for the neutral and ionic nitrogen molecules. Here we report on a significant difference between the emission behavior of the 391-nm line and the other spectral lines under different pump laser polarizations. We attribute this difference to the contribution of the atomic ions to the luminescence emission around 391 nm. The difference becomes more evident in tightly focusing cases, providing an indirect but effective evidence for the dissociation of nitrogen molecular ions.

DOI: 10.1103/PhysRevA.93.013405

I. INTRODUCTION

After filamentation of femtosecond pulses in air, the plasma left behind undergoes complex transitions, emitting characteristic fingerprint luminescence [1]. By measuring the spectroscopy along the propagation path, we cannot only extract the plasma density, electron temperature as well as laser intensity inside filaments [2–5], but also get insight into the excitation and ionization process during the filamentation [6,7]. The backward emission of the plasma luminescence can find promising applications in remote sensing of atmospheric constituents [8,9], and generation of air laser [10,11].

It has been commonly believed that the luminescence from filamentary plasma in air mainly comes from the first negative band system ($B\,^2\Sigma_u{}^+ - X\,^2\Sigma_g{}^+$ transition) of $N_2{}^+$ and the second positive band system ($C\,^3\Pi_u - B\,^3\Pi_g$) of N_2 [12–15]. By far, the origin of nitrogen luminescence, however, remains still an open question, especially that of the luminescence from the second positive band system of N_2 (e.g., 337-nm line). Since the direct high-field photonic excitation of the triplet state N_2 ($C\,^3\Pi_u$) is a spin forbidden process, two possible schemes have been proposed to explain the formation of it. The first scheme is the dissociative recombination through the process: $N_2 + N_2{}^+ \rightarrow N_4{}^+$ followed by $N_4 + e \rightarrow N_2 + N_2(C\,^3\Pi_u)$ [16]; the second one is the collision-assisted intersystem crossing [17]. It seems that the emission mechanism of luminescence from the first negative band system of $N_2{}^+$ is clear, because the excited nitrogen molecular ion $N_2{}^+(B\,^2\Sigma_u{}^+)$ can be generated by the intense laser-induced photoionization of neutral nitrogen molecules.

On another hand, the critical powers for the self-focusing pulse with a different polarization state are different [18], and it is known that the polarization state of laser pulses will have a great influence on the plasma and supercontinuum generation during filamentation [19–21]. Recently, Mitryukovskiy *et al.* have studied the luminescence emission with different laser polarizations experimentally [22,23] and found that there exists a reversal in the relative luminescence intensity between linear and circular polarization with the increase of the pulse energy. To understand the dependence of the luminescence emission on the polarization state of the incident laser pulses, they proposed a new impact excitation channel: Electrons with higher kinetic energy can be produced with circularly polarized laser pulses, leading to the higher population of excited state of $N_2(C\,^3\Pi_u)$ and $N_2{}^+(B\,^2\Sigma_u{}^+)$ via the collision [22].

In this paper, we investigate the influence of laser polarization on the emission of nitrogen characteristic lines during femtosecond filamentation. It is revealed that the nitrogen atoms and atomic ions play a nonignorable role in the luminescence emission, especially for the 391-nm signal, which can well explain the significant difference between the emission behaviors of the 391-nm line and other lines along the propagation axis under different laser polarizations.

II. EXPERIMENTAL DETAILS

The experiment is carried out by using a one-box ultrafast Ti:sapphire amplifier (Coherent Libra) with the wavelength of 800 nm and the width of 50 fs at the repetition rate of 1 kHz. The schematic of experimental setup is shown in Fig. 1. The combination of a half-wave plate and a Glan laser polarizer attenuates laser energy to the desired value. A quarter-wave plate ($\lambda/4$) was installed before the focal lens to change the laser polarization from linear to circular. The produced plasma spectra are first collected by two lenses (BK7 $f = 75$ mm) fixed on a moving stage along the propagation path, and then guided to a spectrometer (Spectra Pro 500i, PI Acton, and the grating is 150 grooves/mm) through the fiber. The plasma luminescence is detected using an intensified charge coupled device (ICCD, PI-MAX, Princeton Instruments) with 1024 × 1024 pixels and a programmable timing generator (DG535, Stanford Research Systems). A rectangular diaphragm (1 mm × 10 mm) is placed 1 mm away from the filament axis to resolve longitudinally the fluorescence signal along the propagation path. Each data point throughout this paper is typically an average of 20 groups of 500 shots' sum so as to reduce the error. The fiber as well as the lenses fixed on the moving stage move back and forth

*amchen@jlu.edu.cn
†mxjin@jlu.edu.cn

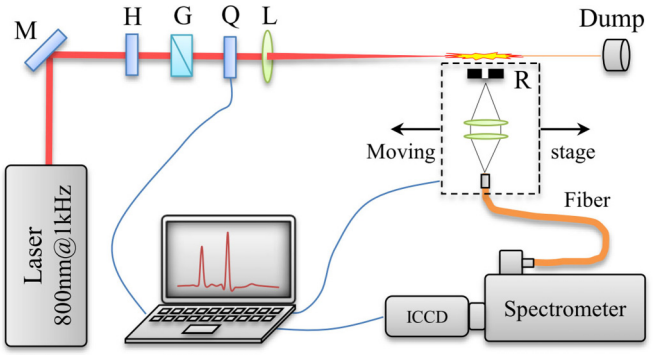

FIG. 1. Schematic of experimental setup for the spectroscopy measurement of filament generated by the femtosecond pulses. F, optical fiber; G, Glan laser polarizer; H, half-wave plate; L, lens; Q, quarter-wave plate; R, rectangular diaphragm.

so as to measure the spectra along the propagation path, where the nearest distances from it to the focusing lens are 35 and 87 cm as their focal lengths are 40 and 100 cm, respectively. For the purpose of facilitating the record of experimental data, this position is set as $z = 0$ mm.

III. RESULTS AND DISCUSSION

Figure 2 present luminescence spectra generated by the circularly (red curves) and linearly polarized (black curves) pulses as the laser energies are 2.0 and 3.1 mJ. The lines marked by 1 refer to the first negative band system of N_2^+ ($B\,^2\Sigma_u^+ \rightarrow X\,^2\Sigma_g^+$ transition) and those marked by 2 refer to the second positive band system of N_2 ($C\,^3\Pi_u \rightarrow B\,^3\Pi_g$ transition). In the transitions $v - v'$, v and v' denote the vibrational levels of upper and lower electronic states, respectively. As is shown in the figure, the 337-, 357-, 380-, and 406-nm lines experience

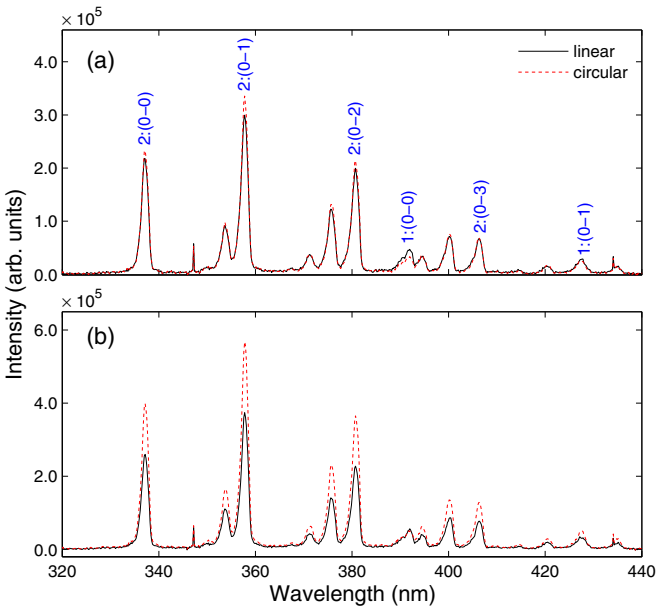

FIG. 2. Spectra generated by the circularly (dashed red curves) and linearly polarized (solid black curves) pulses as the laser energy is (a) 2.0 mJ and (b) 3.1 mJ. The focal length is 100 cm.

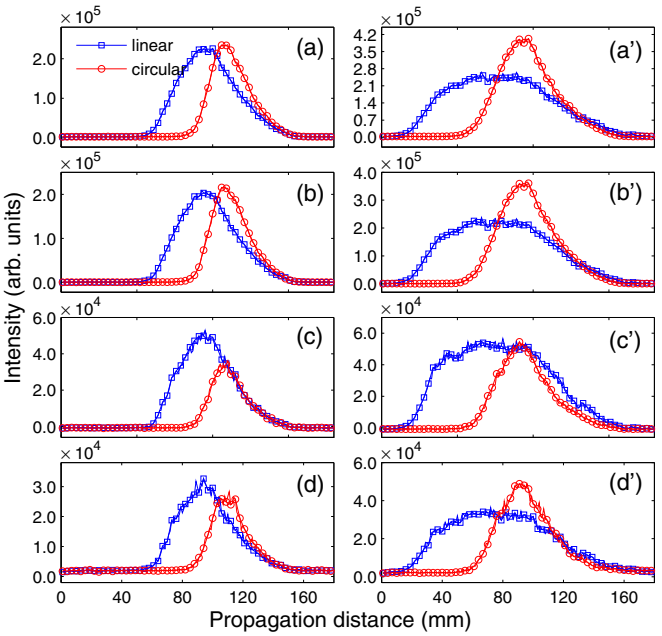

FIG. 3. Variation of the intensity of (a,a′) 337-, (b,b′) 380-, (c,c′) 391-, and (d,d′) 428-nm spectral lines along the propagation axis. The focal length is 100 cm, and the pulse energy is (a)–(d) 2.0 mJ and (a′)–(d′) 3.1 mJ.

the reversal in the relative luminescence intensity between linear and circular polarization, which is found to occur at the same energy. This phenomenon can be attributed to the fact that all these lines come from the second-positive band system of N_2. Since both 391- and 428-nm signals come from the first-negative band system of N_2^+, their emission behaviors are expected to be similar. However, when the laser energy is 3.1 mJ, circular polarization leads to stronger emission of the 428-nm signal while the 391-nm signal is still weaker in the circular polarization case [see Fig. 2(b)], indicating that a different mechanism will be involved in the emission of the 391-nm signal.

Figures 3(a)–3(d) show the variation of the intensities of 337-, 380-, 391-, and 428-nm signals along the propagation axis as the focal length and pulse energy are 100 cm and 2.0 mJ. We can see from the figure that all the spectral lines induced by the same laser polarization show similar variation tendency. For 337- and 380-nm signals, their maximum intensities in the circular and linear polarization cases are almost equal to each other [see Figs. 3(a) and 3(b)]; whereas for 391- and 428-nm signals, the linear polarization leads to the stronger emission [Figs. 3(c) and 3(d)]. As the pulse energy increases to 3.1 mJ, the maximum intensity of 337-, 380- and 428-nm lines are higher in the circular polarization case, as shown by Figs. 3(a′), 3(b′), and 3(d′), while for the 391-nm line, its maximum intensity is almost the same in the two polarization states, as shown by Fig. 3(c′). We have also studied the luminescence emission at lower laser energies; as the energy is below 2.0 mJ, linear polarization leads to stronger emission of all lines, which is consistent with the phenomena observed by Mitryukovskiy *et al.* [22]. It should be noted that along with the increase of pulse energy, the plasma string moves towards

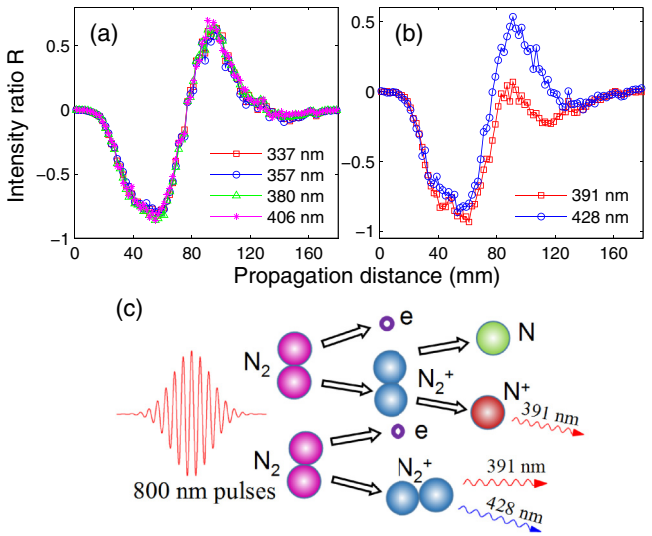

FIG. 4. (a) and (b) Intensity ratio R of different spectral lines as the incident energy is 3.1 mJ and the focal length is 100 cm. (b) Interaction of nitrogen molecules with laser field, resulting in the formation of molecular nitrogen ions, and dissociation of molecular nitrogen ions into nitrogen ions and atoms.

the laser source (see the case of $E_{\text{in}} = 2.0$ and 3.1 mJ), which is a signature of filamentation.

To investigate the luminescence emission in the linear and circular polarization cases more thoroughly, we define the intensity ratio R as

$$R = [I_{\text{circular}}(z) - I_{\text{circular}}(z)]/I_{\text{linear,max}}, \tag{1}$$

where $I_{\text{circular}}(z)$ and $I_{\text{linear}}(z)$ are the luminescence intensities in the circular and linear polarization cases along the filament, and $I_{\text{linear,max}}$ is the maximum of I_{linear} along the propagation axis. In Figs. 4(a) and 4(b), we present the intensity ratio R for different lines along the filament axis. From Fig. 4(a), we can see that the behaviors of 337-, 357-, 380-, and 406-nm lines are in fairly good agreement with each other. This is expected because these lines (corresponding to the transition from the v=0 vibrational state of the $C\,^3\Pi_u$ state to the v=0, 1, 2, 3 vibrational states of the $B\,^3\Pi_g$ state of N_2, respectively) share the same upper level. In contrast, for the 391-nm and 428-nm spectral lines, the behaviors of their intensity ratio R are different from each other. The intensity ratio R of the 391-nm spectral line is lower than zero at most positions, while the behaviors of the intensity ratio R of 428 nm is almost identical to that of the second positive system of N_2, as shown in Fig. 4(b). However, since the 391-nm and 428-nm emission peaks originate from the transition from the $v = 0$ vibrational state of $B\,^2\Sigma_u{}^+$ to v=0, 1 vibrational states of $X\,^2\Sigma_g{}^+$ states of the molecular ion transitions (first-negative system of $N_2{}^+$) [12–15,22], their behaviors along the filament axis upon different laser polarizations are expected to be the same. We have verified that these phenomena still exist in lower energy cases. In the following part, we attempt to analyze this observation in detail.

For the reversal in the relative luminescence intensity between linear and circular polarization upon increasing laser intensity, Mitryukovskiy *et al.* attributed them to the the onset of impact excitation in the case of circularly polarized pulses [22]:

$$N_2(X\,^1\Sigma_g{}^+) + e \rightarrow N_2(C\,^3\Pi_u{}^+) + e, \tag{2}$$

$$N_2(X\,^1\Sigma_g{}^+) + e \rightarrow N_2{}^+(B\,^2\Sigma_u{}^+) + 2e. \tag{3}$$

It is known that the threshold energy of process (2) corresponding to the 337-nm signal is 11 eV, while that of process (3) corresponding to the 391-nm signal is 18.75 eV. Here, we define the energy at which the maximum values of luminescence intensity are the same in the circular and linear polarization states as the "energy threshold." For example, the "energy threshold" for 337 nm is about 2.0 mJ in this case. According to the work of Itikawa [24], the cross section of reaction (2) (337-nm line) is 0.352×10^{-18} cm^2 as the electron energy is 11.23 eV (Table 11 of Ref. [24]), and that of reaction (3) (391-nm line) is 0.103×10^{-18} cm^2 as the electron energy is 19 eV (Table 19 of Ref. [24]). The cross section of the reaction (2) is larger than that of reaction (3) as the kinetic energy of electron is lower than 25 eV [24] and the maximum kinetic energy that the electron can acquire during filamentation is less than this value, indicating that the former is much larger than the later as the electron kinetic energy is the same. This can well interpret the phenomena that the energy threshold for the signals from $N_2{}^+$ (391 and 428 nm) is higher than that for the signals from N_2 (337, 357, 380, and 406 nm, etc.). As is known, along with the increase of input pulse energy, the pondermotive energy of electron ionized increase. Therefore, as the pulse energy increase from 2 to 3.1 mJ, the impact excitation in the case of circularly polarized pulses will be enhanced greatly, resulting in the reversal in the relative luminescence intensity between linear and circular polarization. According to this impact excitation of the nitrogen ions $N_2{}^+$, we expect that 391 and 428 nm present the similar dependence on pump laser polarization along z, since they share the upper level of emission. However, our experimental observation do not agree with this expectation.

In effect, we notice that for the 391-nm signal, its component is complicated: Apart from molecular nitrogen ions $N_2{}^+$, excited nitrogen ions N_{II} also contribute to its emission (there exists strong light emission at 391.39, 391.54, and 391.55 nm) [25]. However, since the linewidth of the component from the molecular nitrogen ions is too broad, which covers the component from the atomic nitrogen ions, they cannot be distinguished due to the limited spectral resolution in our current experiment and that of others [3]. It is well known that during the filamentation, N_2 and $N_2{}^+$ will undergo the dissociation process due to the high intensity of the laser pulse, thus generating nitrogen atoms and nitrogen ions [24], as illustrated in Fig. 3(c) (here we just consider the dissociation of $N_2{}^+$). Furthermore, the component from N_{II} is more intense (e.g., $^3D^{\text{o}} - ^3P$; transition strength: $A_{k,i} = 3.22 \times 10^7$ s^{-1} [25]), which surpasses that from $N_2{}^+$ (transition strength: $A_{0,0} = 1.14 \times 10^7$ s^{-1}) [12]. For the emission from N_{II}, a larger signal would be generated with a linearly polarized pump. For the luminescence emission from nitrogen molecular ions $N_2{}^+$ excited by electron collisions, the circularly polarized pump laser should produce a stronger signal [22]. In view

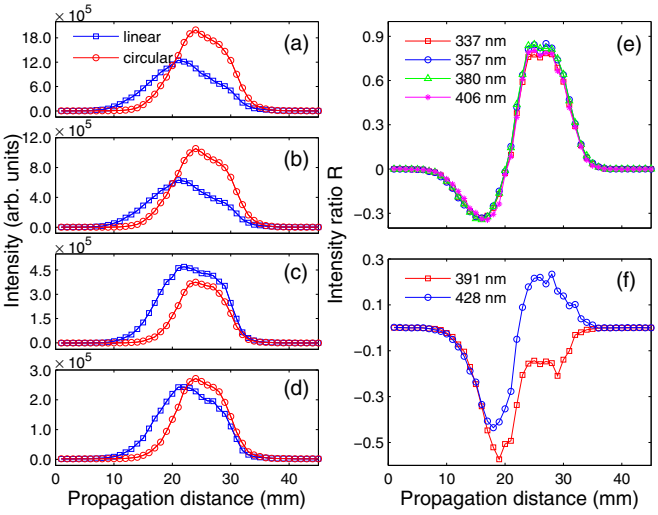

FIG. 5. Variation of the intensity of (a) 337-, (b) 380-, (c) 391-, and (d) 428-nm spectral lines along the propagation axis. (e) and (f) Intensity ratio R of different spectral lines. The focal length is 40 cm, and the pulse energy is 3.1 mJ.

of our observation, we speculate the emission from N_{II} contributes more importantly to the spectrum around 391 nm. As a whole, the 391-nm signal is more intense in the linear polarization case. Though N_I or N_{II} also contributes to the emission of other lines (428 nm included), the component from the N_I or N_{II} is much weaker than that from N_2 or N_2^+, therefore, impact excitation dominates their emission. On the other hand, along with the increase of laser energy, the laser intensity inside the filament will not increase constantly but be clamped to a certain value ($I_{clamp} \simeq 5 \times 10^{17}$ W/m^2), and the ionization rate is confined to a certain value [26]. Under this circumstance, the component from N_{II} will no longer increase due to the limited number of N_{II}, whereas, the impact excitation has no such limitation. Consequently, impact excitation will dominate the emission of the 391-nm signal gradually, and it becomes independent of laser polarization at higher energy. It is the competition between the emission from the N_{II} and impact excitation that results in the different behavior of the 391-nm signal under different polarizations.

It is well known that the plasma density will increase with the decrease of the focal length of external lens [27,28]. The dissociation of N_2 and N_2^+ will be enhanced in tightly focusing conditions, generating more nitrogen atoms and ions. The luminescence emission from the generated nitrogen atoms and ions will be more intense in the linear polarization state, therefore, we can infer that the difference between the emission behaviors of the 391-nm as well as the 428-nm lines and the other spectral lines along the propagation axis will be more evident. To verify this assumption, we carry out the same experiment in the shorter focal length case ($f = 40$ cm), as shown in Fig. 5. Compared with the results shown in Figs. 3(a′)–3(d′), for the 337- and 380-nm signals, their emission is still more intense in the circular polarization state, similar to that shown in Figs. 3(a′) and 3(b′) [see Figs. 5(a) and 5(b)], while for the 391-nm signal, its emission is more intense in the linear polarization state [see Fig. 5(c)], which

TABLE I. Amplification ratios I_s/I_l (linear) and I_s'/I_l' (circular) for different lines as the pulse energy is 3.1 mJ. I_s and I_l denote the maximum spectrum intensity in shorter and longer focal length cases.

Line (nm)	337	357	380	391	406	428
I_s/I_l	4.80	3.64	2.69	8.61	2.95	7.14
I_s'/I_l'	4.96	3.93	2.89	6.88	2.90	5.55

is quite different from that shown in Fig. 3(c′), although the pulse energy is the same in both cases. The difference between the luminescence emission behaviors in different polarization states in the tightly focusing cases can be clearly seen from Figs. 5(e) and 5(f). It can be seen from the figure that the intensity ratios of the 337-, 357-, 380-, and 406-nm signals are still in fairly good agreement with each other, while for those of the 391- and 428-nm signals, the difference between them becomes more obvious. Compared with the longer focal length cases, the intensity ratio R for the 428-nm signal also becomes different from those for the lines from the second positive system of excited N_2, which can be attributed to the threshold energy of impact excitation from circularly polarized pulses for lines from excited N_2^+ is much higher compared with that for lines from the excited N_2 [22]. The above study provides an indirect but effective evidence for the dissociation of nitrogen molecular ions, thus confirming our conclusion. It should be noted that the plasma density will not increase with the decrease of the focal length of the external lens constantly but be limited to an extent: Air is fully ionized [29], which corresponds to a transition from a filament to a laser-gas interaction regime [30]. It is believed that the phenomena observed still exist in the limited cases, for the only required condition is the generation of plasmas in air. However, since we focus on the phenomenon of cavity-free lasing in the atmosphere which will be helpful to the remote sensing, femtosecond filamentation is the most promising approach owing to the fact that femtosecond laser pulses are suitable for long-distance propagation. Therefore, in our work, we just investigate the plasma luminescence emission in the filament regime.

In addition, the intensity of the lines from the second positive system of N_2 increases about three times as the focal length changes from 100 to 40 cm, and that for 428 nm increases about seven times while for the 391-nm signal, its intensity increases about nine times in linear polarization, as shown in Table I. It can be seen from the table that the molecular nitrogen ions lead to the stronger luminescence emission, and in a recent letter, Liu *et al.* proposed the recollision induced superradiance to illustrate this phenomena [31]. It has been reported that the self-seeded amplification plays a significant role in the generation of 391- and 428-nm signals [31–33]. However, they also rate that the 391 nm comes from excited N_2^+, the difference between the emission behaviors of it and the 428-nm signal cannot be explained.

IV. CONCLUSION

In conclusion, the laser polarization state has a great influence on the evolution of fluorescence emission along the

propagation axis: The circular polarization leads to stronger fluorescence emission, providing the pulse energy is high enough. By measuring the plasma luminescence spectra under linear and circular polarizations along the propagation axis, we find that the emission behavior of the 391-nm signal is different from those of the other lines (including the 428-nm one) under different polarizations. Analyzing the origin of spectral lines, we can find the answer: During femtosecond filamentation, nitrogen atoms, and atomic ions generated due to the dissociation of nitrogen molecules and molecular ions emit luminescence in the UV range, in particular, the spectra from the nitrogen atomic ion N_{II} overlap with that from the excited nitrogen molecular ions N_{II}^{+} at 391 nm. It is the competition between the emission from the N_{II} and impact excitation that makes the difference between the emission behavior of the 391-nm signal and those of the other lines under different polarizations. The dissociation of nitrogen molecules and molecular ions is enhanced in tightly focusing conditions, making the difference more obvious. These studies indicate that nitrogen atoms and ions play a significant role in the luminescence emission during femtosecond filamentation, especially in the tightly focusing cases.

ACKNOWLEDGMENTS

We acknowledge the support from the National Basic Research Program of China (973 Program, Grant No. 2013CB922200), the National Natural Science Foundation of China (Grants No. 11474129 and No. 11504129), the Research Fund for the Doctoral Program of Higher Education in China (Grant No. 20130061110021), the China Postdoctoral Science Foundation (Grant No. 2014M551169), and the Graduate Innovation Fund of Jilin University (Grant No. 2015091).

[1] S. L. Chin, H. L. Xu, Q. Luo, F. Théberge, W. Liu, J. F. Daigle, Y. Kamali, P. T. Simard, J. Bernhardt, S. A. Hosseini, M. Sharifi, G. Méjean, A. Azarm, C. Marceau, O. Kosareva, V. P. Kandidov, N. Aközbek, A. Becker, G. Roy, P. Mathieu, J. R. Simard, M. Châteauneuf, and J. Dubois, Appl. Phys. B **95**, 1 (2009).
[2] S. Xu, X. Sun, B. Zeng, W. Chu, J. Zhao, W. Liu, Y. Cheng, Z. Xu, and S. L. Chin, Opt. Express **20**, 299 (2012).
[3] J. Bernhardt, W. Liu, F. Théberge, H. L. Xu, J. F. Daigle, M. Chateâuneuf, J. Dubois, and S. L. Chin, Opt. Commun. **281**, 1268 (2008).
[4] S. A. Hosseini, Q. Luo, B. Ferland, W. Liu, N. Aközbek, G. Roy, and S. L. Chin, Appl. Phys. B **77**, 697 (2003).
[5] L. Shi, W. Li, Y. Wang, X. Lu, L. Ding, and H. Zeng, Phys. Rev. Lett. **107**, 095004 (2011).
[6] J. Yao, H. Xie, B. Zeng, W. Chu, G. Li, J. Ni, H. Zhang, C. Jing, C. Zhang, H. Xu, Y. Cheng, and Z. Xu, Opt. Express **22**, 19005 (2014).
[7] J.-F. Daigle, A. Jaroń-Becker, S. Hosseini, T.-J. Wang, Y. Kamali, G. Roy, A. Becker, and S. L. Chin, Phys. Rev. A **82**, 023405 (2010).
[8] J. Kasparian, M. Rodriguez, G. Méjean, J. Yu, E. Salmon, H. Wille, R. Bourayou, S. Frey, Y.-B. André, A. Mysyrowicz, R. Sauerbrey, J.-P. Wolf, and L. Wöste, Science **301**, 61 (2003).
[9] H. L. Xu and S. L. Chin, Sensors **11**, 32 (2010).
[10] A. Laurain, M. Scheller, and P. Polynkin, Phys. Rev. Lett. **113**, 253901 (2014).
[11] H. Zhang, C. Jing, J. Yao, G. Li, B. Zeng, W. Chu, J. Ni, H. Xie, H. Xu, S. L. Chin, K. Yamanouchi, Y. Cheng, and Z. Xu, Phys. Rev. X **3**, 041009 (2013).
[12] F. R. Gilmore, R. R. Laher, and P. J. Espy, J. Phys. Chern. Ref. Data **21**, 1005 (1992).
[13] A. Talebpour, M. Abdel-Fattah, A. D. Bandrauk, and S. L. Chin, Laser Physics **11**, 68 (2001).
[14] A. N. Wright and C. A. Winkler, *Active Nitrogen* (Academic, New York, 1968).
[15] G. N. Gibson, R. R. Freeman, and T. J. McIlrath, Phys. Rev. Lett. **67**, 1230 (1991).
[16] H. L. Xu, A. Azarm, J. Bernhardt, Y. Kamali, and S. L. Chin, Chem. Phys. **360**, 171 (2009).
[17] B. R. Arnold, S. Roberson, and P. M. Pellegrino, Chem. Phys. **405**, 9 (2012).
[18] J. H. Marburger, Prog. Quantum Electron. **4**, 35 (1975).
[19] M. Kolesik, J. V. Moloney, and E. M. Wright, Phys. Rev. E **64**, 046607 (2001).
[20] G. Fibich and B. Ilan, Phys. Rev. Lett. **89**, 013901 (2002).
[21] G. Fibich and B. Ilan, Phys. Rev. E **67**, 036622 (2003).
[22] S. Mitryukovskiy, Y. Liu, P. Ding, A. Houard, A. Couairon, and A. Mysyrowicz, Phys. Rev. Lett. **114**, 063003 (2015).
[23] P. Ding, S. Mitryukovskiy, A. Houard, E. Oliva, A. Couairon, A. Mysyrowicz, and Y. Liu, Opt. Express **22**, 29964 (2014).
[24] Y. Itikawa, J. Phys. Chem. Ref. Data **35**, 31 (2006).
[25] http://physics.nist.gov/PhysRefData/ASD/lines_form.html.
[26] A. Couairon and A. Mysyrowicz, Phys. Rep. **441**, 47 (2007).
[27] Y.-H. Chen, S. Varma, T. M. Antonsen, and H. M. Milchberg, Phys. Rev. Lett. **105**, 215005 (2010).
[28] F. Théberge, W. Liu, P. T. Simard, A. Becker, and S. L. Chin, Phys. Rev. E **74**, 036406 (2006).
[29] P. P. Kiran, S. Bagchi, S. R. Krishnan, C. L. Arnold, G. R. Kumar, and A. Couairon, Phys. Rev. A **82**, 013805 (2010).
[30] K. Lim, M. Durand, M. Baudelet, and M. Richardson, Sci. Rep. **4**, 7217 (2014).
[31] Y. Liu, P. Ding, G. Lambert, and A. Houard, Phys. Rev. Lett. **115**, 133203 (2015).
[32] W. Chu, G. Li, H. Xie, J. Ni, J. Yao, B. Zeng, H. Zhang, C. Jing, H. Xu, Y. Cheng, and Z. Xu, Laser Phys. Lett. **11**, 015301 (2014).
[33] C. Jing, H. Zhang, W. Chu, H. Xie, J. Ni, Bin Zeng, G. Li, J. Yao, H. Xu, Y. Cheng, and Z. Xu, Opt. Express **22**, 3151 (2014).